JOC*Article*

# Emission from Charge Recombination during the Pulse Radiolysis of 9-Cyano-10-phenylethynylanthracenes with Donor and Acceptor Substituents

Shingo Samori,[†] Sachiko Tojo,[†] Mamoru Fujitsuka,[†] Hua-Jyu Liang,[‡] Tong-Ing Ho,[‡] Jye-Shane Yang,[‡] and Tetsuro Majima[†,*]

*The Institute of Scientific and Industrial Research (SANKEN), Osaka University, Mihogaoka 8-1, Ibaraki, Osaka 567-0047, Japan, and Department of Chemistry, National Taiwan University, Taipei, Taiwan 10617*

*majima@sanken.osaka-u.ac.jp*

*Received May 4, 2006*



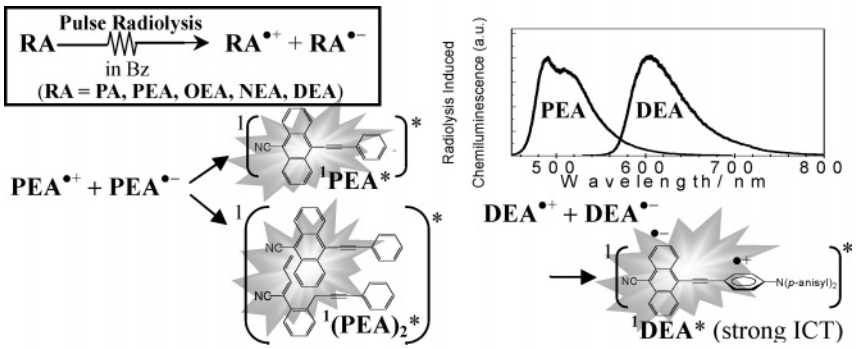


Emission from 9-cyano-10-phenylanthracene and 9-cyano-10-phenylethynylanthracenes having donor and acceptor substituents (**RA** = **PA**, **PEA**, **OEA**, **NEA**, and **DEA**) was studied with the time-resolved fluorescence measurement during the pulse radiolysis of **RAs** in benzene (Bz). **PA** and **DEA** showed only monomer emission, while other **RAs** (**PEA**, **OEA**, and **NEA**) showed both monomer and excimer emissions with much lower intensities. On the basis of the steady-state and transient absorption and emission measurements, the formation of **RA** in the singlet excited state ($^1$**RA**$^*$) can be attributed to the charge recombination between **RA** radical cation and anion (**RA**$^{\bullet+}$ and **RA**$^{\bullet-}$, respectively) which are initially generated from the radiolytic reaction in Bz. It is expected that for **PA** with a twisted geometry, the charge recombination between **PA**$^{\bullet+}$ and **PA**$^{\bullet-}$ occurs to give $^1$**PA**$^*$ during the pulse radiolysis in Bz. For **PEA** and **OEA**, $\pi$-stacking interaction is possible for the formation of an encounter complex during the charge recombination between **RA**$^{\bullet+}$ and **RA**$^{\bullet-}$. For **NEA**, it is expected that **NEA**$^{\bullet+}$ and **NEA**$^{\bullet-}$ collide neck-to-neck to generate the excimer due to the twisted geometry. For **DEA**, a considerably twisted structure is assumed to give $^1$**DEA**$^*$ with strong ICT character but not $^1$(**DEA**)$_2^*$ because of the bulky donor substituent.

## Introduction

Charge recombination of radical cation (**M**$^{\bullet+}$) and anion (**M**$^{\bullet-}$), which are generated by electrolysis of organic molecule (**M**) in solution, leads to the formation of electronically excited states of **M** such as $^1$**M**$^*$ and/or the singlet excimer of $^1$**M**$^*$ ($^1$**M**$_2^*$) on the electrode surfaces. Since $^1$**M**$^*$ and $^1$**M**$_2^*$ emit the fluorescence, it is called electrogenerated chemiluminescence (ECL).[1−5] The formation of excited states in the solid state by the application of an electric field (as in OLED) has been shown to follow a mechanism similar to that in solution (ECL).[4] Recently, organic $\pi$-conjugated donor−acceptor (D−A) type **M** has attracted considerable attention as electroluminescent

* To whom correspondence should be addressed. Telephone: Japan +6-6879-8495. Fax: Japan +6-6879-8499.
[†] Osaka University.
[‡] National Taiwan University.

(1) (a) Faulkner, L. R.; Bard, A. J. *Electroanalytical Chemistry*; Marcel Dekker: New York, 1977; Vol. 10, pp 1−95. (b) Bard, A. J.; Faulkner, L. R. *Electrochemical Methods Fundamentals and Applications*, 2nd ed.; John Wiley and Sons: New York, 2001, pp 736−745. (c) Richter, M. M. *Chem. Rev.* **2004**, *104*, 3003.

10.1021/jo060929n CCC: $33.50 
Published on Web 10/18/2006

**SCHEME 1**

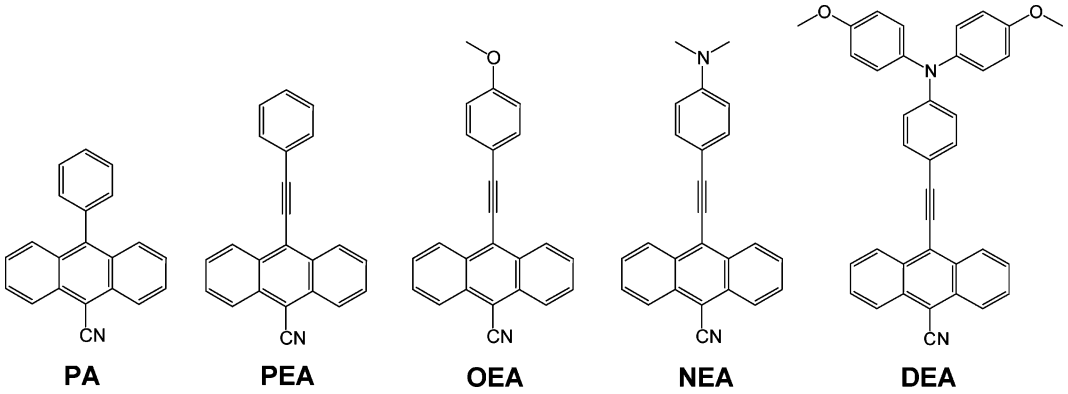


materials for OLEDs.[6] ECL from the D−A type **M** can originate from the locally excited states of D or A moiety, the intramolecular charge transfer (ICT) states,[2−3,5a−c] or even from intermolecular excimers or exciplexes.[2−3,5d,e] Thus, a judicious choice of the D/A unit could allow the control of the HOMO/LUMO levels and the emission color of the D−A type **M**. However, most luminescent materials are highly emissive in their dilute solutions but become weakly luminescent when in concentrated solutions or fabricated into thin films. Under these conditions, the molecules aggregate to form less emissive species such as excimers, leading to a reduction in the luminescence efficiency. When the Stokes shift is small, the luminescence efficiency is also reduced due to self-absorption as a result of high concentration of **M** needed to obtain the measurable emission. For some D−A type **Ms**, the ICT ECL was observed at longer wavelengths than that from the locally excited state, reducing the self-absorption.[2,3]

In our previous papers, we proposed the emission mechanisms of D−A type **M** with an ethynyl linkage (**RE**) such as donor-substituted phenylquinolinylethynes,[7a] phenyl(9-acridinyl)-ethynes,[7b] phenyl(9-cyanoanthracenyl)ethynes,[7b] and arylethynylpyrenes[7c] during pulse radiolysis in benzene (Bz). Some of these compounds are known as ECL-active **M**.[2] On the basis of the transient absorption and emission measurements and steady-state measurements, the formation of D−A type **RE** in the singlet excited state ($^1$**RE**$^*$) and/or singlet excimer ($^1$**RE**$_2^*$) can be attributed to the charge recombination between **RE**$^{\bullet+}$ and **RE**$^{\bullet-}$ which are generated initially from the radiolytic reaction in Bz. The emission mechanism of **RE** in pulse radiolysis strongly depends on the charges resulted from the presence of electron donating- or withdrawing substituents.[7] In addition, it is found that the presence or absence of excimer emission depends on the geometries of **RE**.

In this paper, we report the emission from the charge recombination between **RA**$^{\bullet+}$ and **RA**$^{\bullet-}$ of $\pi$-conjugated D−A type molecules having 9-cyanoanthracenyl as the electron acceptor moiety (**RAs**); 9-cyano-10-phenylanthracene (**PA**), 9-cyano-10-phenylethynylanthracene (**PEA**), and various 9-cyano-10-(donor-substituted phenylethynyl)anthracenes with methoxy- (ie., anisole, **OEA**), *p*-*N*,*N*-(dimethylamino)- (**NEA**), and *N*,*N*-di-*p*-anisylamino- (**DEA**) groups as donor moieties, because **RA** are known as the ECL-active molecules in $CH_2Cl_2$.[3] Using pulse radiolysis technique, both **RA**$^{\bullet+}$ and **RA**$^{\bullet-}$ can be generated at the same time in Bz. Therefore, it is expected that $^1$**RA**$^*$, $^3$**RA**$^*$, and/or $^1$(**RA**)$_2^*$ can be generated from the charge recombination between **RA**$^{\bullet+}$ and **RA**$^{\bullet-}$ during the pulse radiolysis of **RA** in Bz. The emission from **PA** with no ethynyl linkage is also examined in order to compare with that from other **RA** with an ethynyl linkage. The time-resolved transient absorption and emission measurements during the pulse radiolysis of the ECL-active **Ms** in solution were useful to gain a better understanding of their emission mechanism, providing valuable information for the molecular design with an efficient luminescence character.

## Results and Discussion

Scheme 1 depicts the chemical structures of $\pi$-conjugated D−A type molecules having a 9-cyanoanthracenyl moiety (**PA**, **PEA**, **OEA**, **NEA**, and **DEA**). For 9-cyano-10-(donor-substituted phenylethynyl)anthracenes (**OEA**, **NEA**, and **DEA**), their electron-donating character of the substituents (methoxy-, *p*-*N*,*N*-(dimethylamino)-, and *N*,*N*-di-*p*-anisylamino-groups, respectively) increases in this order.[3]

(2) (a) Elangovan, A.; Chen, T.-Y.; Chen, C.-Y.; Ho, T.-I. *Chem. Commun.* **2003**, 2146. (b) Elangovan, A.; Yang, S.-W.; Lin, J.-H.; Kao, K.-M.; Ho, T.-I. *Org. Biomol. Chem.* **2004**, *2*, 1597. (c) Elangovan, A.; Chiu, H.-H.; Yang, S.-W.; Ho, T.-I. *Org. Biomol. Chem.* **2004**, *2*, 3113. (d) Elangovan, A.; Kao, K.-M.; Yang, S.-W.; Chen, Y.-L.; Ho, T.-I.; Su, Y. O. *J. Org. Chem.* **2005**, *70*, 4460. (e) Yang, S.-W.; Elangovan, A.; Hwang, K.-C.; Ho, T.-I. *J. Phys. Chem. B* **2005**, *109*, 16628.

(3) Lin, J.-H.; Elangovan, A.; Ho, T.-I. *J. Org. Chem.* **2005**, *70*, 7397.

(4) (a) Anderson, J. D.; McDonald, E. M.; Lee, P. A.; Anderson, M. L.; Ritchie, E. L.; Hall, H. K.; Hopkins, T.; Padias, A.; Thayumanavan, S.; Barlow, S.; Marder, S. R.; Jabbour, G. E.; Shaheen, S.; Kippelen, B.; Peyghambarian, N.; Wightman, R. M.; Armstrong, N. R.; Mash, E. A.; Wang, J. *J. Am. Chem. Soc.* **1998**, *120*, 9646. (b) Armstrong, N. R.; Anderson, J. D.; Lee, P. A.; McDonald, E. M.; Wightman, R. M.; Hall, H. K.; Hopkins, T.; Padias, A.; Thayumanavan, S.; Barlow, S.; Marder, S. R. *SPIE* **1999**, *3476*, 178. (c) Armstrong, N. R.; Whightman, R. M.; Gross, E. M. *Annu. Rev. Phys. Chem.* **2001**, *52*, 391.

(5) (a) Lai, R. Y.; Kong, X.; Jenekhe, S. A.; Bard, A. J. *J. Am. Chem. Soc.* **2003**, *125*, 12631. (b) Kapturkiewicz, A. *Chem. Phys.* **1992**, *166*, 259. (c) Kawai, M.; Itaya, K.; Toshima, S. *J. Am. Chem. Soc.* **1980**, *84*, 2368. (d) Lai, R. Y.; Fleming, J. J.; Merner, B. L.; Vermeij, R. J.; Bodwell, G. J.; Bard, A. J. *J. Phys. Chem. A.* **2004**, *108*, 376. (e) Strau$\beta$, J.; Daub, J. *Adv. Mater.* **2002**, *14*, 1652.

(6) (a) Goes, M.; Verhoeven, J. W.; Hofstraat, H.; Brunner, K. *ChemPhysChem* **2003**, *4*, 349. (b) Thomas, K. R. J.; Lin, J. T.; Tao, Y.-T.; Chuen, C.-H. *Chem. Mater.* **2002**, *14*, 3852. (c) Zhu, W.; Hu, M.; Yao, R.; Tian, H. *J. Photochem. Photobiol., A* **2003**, *154*, 169. (d) Thomas, K. R. J.; Lin, J. T.; Velusamy, M.; Tao, Y.-T.; Chuen, C.-H. *Adv. Funct. Mater.* **2004**, *14*, 83. (e) Chiang, C.-L.; Wu, M.-F.; Dai, D.-C.; Wen, Y.-S.; Wang, J.-K.; Chen, C.-T. *Adv. Funct. Mater.* **2005**, *15*, 231.

(7) (a) Samori, S.; Hara, M.; Tojo, S.; Fujitsuka, M.; Yang, S.-W.; Elangovan, A.; Ho, T.-I.; Majima, T. *J. Phys. Chem. B.* **2005**, *109*, 11735. (b) Samori, S.; Tojo, S.; Fujitsuka, M.; Yang, S.-W.; Elangovan, A.; Ho, T.-I.; Majima, T. *J. Org. Chem.* **2005**, *70*, 6661. (c) Samori, S.; Tojo, S.; Fujitsuka, M.; Yang, S.-W.; Ho, T.-I.; Yang, J.-S.; Majima, T. *J. Phys. Chem. B* **2006**, *110*, 13296−13303.

**TABLE 1. Photophysical Properties of RA in $CH_2Cl_2$, Hexane, and Bz[a]**

| | in $CH_2Cl_2$ | | | in hexane | | | in Bz | | | |
|---|---|---|---|---|---|---|---|---|---|---|
| **RA** | $\lambda$ max(Abs), nm | $\lambda$ max(Fl ), nm | $\phi_{fl}$ | $\lambda$ max(Abs), nm | $\lambda$ max(Fl), nm | $\phi_{fl}$ | $\lambda$ max(Abs), nm | $\lambda$ max(Fl), nm | $\phi_{fl}$ | $\tau_{fl}$[b], ns |
| **PA** | 391 (411) | 455 | 0.28 | 385 (496, 366) | 420 (442) | 0.56 | 389 (413, 368) | 454 (432) | 0.37 | 6.0 |
| **PEA** | 421 (446) | 488 | 0.48 | 415 (440) | 446 (473) | 0.54 | 422 (446) | 461 (487) | 0.45 | 5.1 |
| **OEA** | 431 (453) | 485 | 0.41 | 455 (484) | 455 (484) | 0.52 | 430 (453) | 473 (500) | 0.43 | 4.1 |
| **NEA** | 482 | 584 | 0.06 | 493 (518) | 493 (518) | 0.32 | 479 | 557 | 0.19 | 4.0 |
| **DEA** | 491 | 557 | 0 | 517 | 517 | 0.25 | 490 | 589 | 0.11 | 4.8 |

[a] Although $\phi_{fl}$ values for RA have been determined in ref 3, they were found to be incorrect because of a mistake. Therefore, they were carefully redetermined in the present study. The values in parentheses are the maxima of vibrational peaks. [b] The fluorescence lifetime.

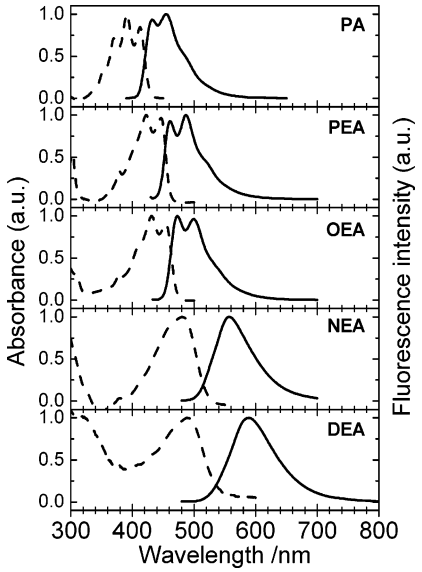


**FIGURE 1.** Absorption (broken line) and fluorescence (solid line) spectra obtained by the steady-state absorption and fluorescence measurement of **RA** in Ar-saturated Bz ($10^{-5}$ M).

**Photophysical and Electrochemical Properties.** The photophysical properties of **RAs** in $CH_2Cl_2$ ($\epsilon = 9.08$), hexane ($\epsilon = 1.89$), and Bz ($\epsilon = 2.28$) are listed in Table 1. The ground-state absorption spectra of **PA**, **PEA**, and **OEA** in these solvents showed the structured $\pi-\pi^*$ transition region around 400−420 nm which can be attributed to the local excitation of the 9-cyanoanthracenyl chromophore. On the other hand, those of **NEA** and **DEA** clearly showed the structureless band around 480 nm which can be attributed to the charge-transfer transition. The absorption peaks of **RAs** in these solvents showed little dependence on the solvent polarity. However, the fluorescence peaks of **RA** in $CH_2Cl_2$ or Bz were observed at longer wavelengths than those in hexane due to the solvent polarity (Table 1 and Figure 1). **OEA** has been found to have a weak intramolecular charge transfer (ICT) character in the excited state because a red shift was observed in several other solvents such as Bz, THF, $CH_2Cl_2$, acetone, EtOH, MeOH, $CH_3CN$, and DMSO.[3] On the other hand, the strong ICT is reasonably assumed for **NEA** and **DEA**. In Bz, D−A type **RA** (**OEA**, **NEA**, and **DEA**) also showed a red shift of the emission maxima. Therefore, the ICT is also assumed for D−A type **RA** in Bz, but not in hexane.

The electrochemical properties of **RA** in $CH_2Cl_2$ are listed in Table 2. Using a setup consisting of fluorescence spectrophotometer and voltammograph with a PC interface, ECL emissions of **RA** were observed with peaks at 456−588 nm in the presence of 0.05 M tetrabutylammonium perchlorate (TBAP) as supporting electrolyte.[3] The ECL emission maxima for **PA** and **NEA** in $CH_2Cl_2$ (Table 2) are very close to the fluorescence maxima (Table 1).

**TABLE 2. Electrochemical Properties of RA in $CH_2Cl_2$[a]**

| | in $CH_2Cl_2$ | | | | |
|---|---|---|---|---|---|
| | | | | $\lambda$ max(EC L) | |
| **RA** | $E_{ox}$, V | $E_{red}$, V | -$\Delta H°$, eV | nm | eV |
| **PA** | 1.80 | −1.55 | 3.19 | 456 | 2.72 |
| **PEA** | 1.14 | −1.24 | 2.22 | 552 | 2.25 |
| **OEA** | 1.10 | −1.32 | 2.26 | 547 | 2.27 |
| **NEA** | 0.97 | −1.35 | 2.16 | 588 | 2.11 |
| **DEA** | 0.90 | −1.29 | 2.03 | 643 | 1.93 |

[a] Reference 3 except for the $E_{ox}$ value of OEA (1.10 V) and the singlet excited-state energy calculated from the ECL emission maximum of DEA which were measured in this study.

To elucidate the ECL emission mechanism, the annihilation enthalpy change ($-\Delta H°$) for the charge recombination between the radical cation ($\mathbf{M}^{\bullet+}$) and radical anion ($\mathbf{M}^{\bullet-}$) is calculated by eq 1,[8]

$$-\Delta H° = [(E_{ox} - E_{red})]^{\epsilon_s} - \Delta G_{sol}{}^{\epsilon_s} - w_{a,\mu} + T\Delta S° \quad (1)$$

where $E_{ox}$ and $E_{red}$ are the oxidation and reduction potentials of the solute molecule (**M**), respectively. $\epsilon_s$, $\Delta G_{sol}$, and $w_{a,\mu}$ represent the static dielectric constant of solvent, the free energy change of solvation, and the work required to bring $\mathbf{M}^{\bullet+}$ and $\mathbf{M}^{\bullet-}$ within a likely separation distance, respectively. In $CH_2Cl_2$, $-\Delta H°$ can be expressed using $E_{ox}$ and $E_{red}$ measured in $CH_2Cl_2$ by simplified eq 2,[3]

$$-\Delta H° = E_{ox} - E_{red} - 0.16\ \text{eV} \quad (2)$$

The calculated $-\Delta H°$ values for **RA** are listed in Table 2. $-\Delta H°$ for **PA**, **NEA**, and **DEA** are sufficiently larger than the singlet excited-state energies calculated from the ECL emission maxima, and hence, $^1$**PA**$^*$, $^1$**NEA**$^*$, and $^1$**DEA**$^*$ can be generated from the charge recombination between $\mathbf{RA}^{\bullet+}$ and $\mathbf{RA}^{\bullet-}$ (S-route). On the other hand, $-\Delta H°$ for **PEA** and **OEA** are not sufficiently larger than the energies of the ECL emission maxima. Therefore, it is suggested that initially $^3$**RA**$^*$ is generated to be followed by triplet−triplet annihilation giving $^1$**RA**$^*$ (T-route).

**Emission Spectra Observed during the Pulse Radiolysis of RA in Bz.** The time-resolved emission spectra were observed to show a monotonic decay after an electron pulse during the pulse radiolysis of **RA** (5 and 10 mM) in Ar-saturated Bz. At 10 mM, all **RA** showed the emission maxima at 471−680 nm during pulse radiolysis (Figure 2). For **PEA**, **OEA**, and **NEA**,

(8) Gross, E. M.; Anderson, J. D.; Slaterbeck, A. F.; Thayumanavan, S.; Barlow, S.; Zhang, Y.; Marder, S. R.; Hall, H. K.; Nabor, M. F.; Wang, J.-F.; Mash, E. A.; Armstrong, N. R.; Wightman, R. M. *J. Am. Chem. Soc.* **2000**, *122*, 4972.

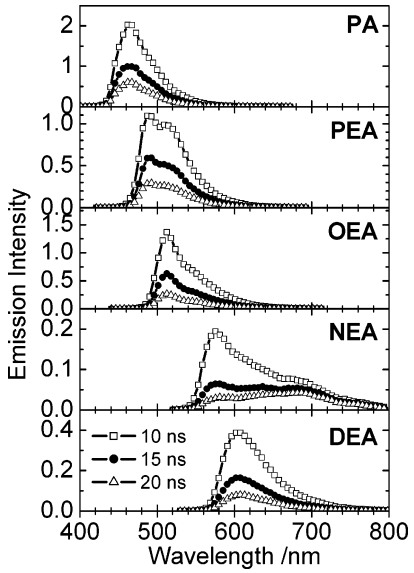


**FIGURE 2.** Emission spectra recorded at time $t = 10$ (open square), 15 (solid circle), and 20 (open triangle) ns after an electron pulse during the pulse radiolysis of **RA** in Ar-saturated Bz (10 mM).

**TABLE 3. Emission Maxima ($\lambda^{Em}$) and Relative Emission Intensity during the Pulse Radiolysis of RA in Ar-Saturated Bz (5 and 10 mM)**

| | radiolysis-induced chemiluminescence | | | |
|---|---|---|---|---|
| | 5 mM | | 10 mM | |
| **RA** | $\lambda^{Em}$, nm | relative intensity (%)[a] | $\lambda^{Em}$, nm | relative intensity (%)[a] |
| **PA** | 468 | 100 | 471 | 86.1 |
| **PEA** | 495 | 49.8 | 491, 510[b] | 49.6 |
| **OEA** | 507 | 38.4 | 513, 550[b] | 45.9 |
| **NEA** | 568 | 15.0 | 576, 680[b] | 10.6 |
| **DEA** | 600 | 12.6 | 608 | 15.8 |

[a] Relative to the emission intensity for PA in Ar-saturated Bz. Emission intensity was determined from the total amount of emission. [b] Excimer emission.

another emission maximum was observed at a longer wavelength side during pulse radiolysis and was assigned to the excimer emission,[7] which was not observed in the steady-state fluorescence measurement even at a high concentration. Because the fluorescence maxima of the D−A type **RAs** (**OEA**, **NEA**, and **DEA**) were observed at longer wavelength side than that of **PEA**, an emissive ICT is indicated for the D−A type **RAs** during pulse radiolysis in Bz. In addition, the shape of the emission spectra of **PA**, **PEA**, and **OEA** were different from those observed in the steady-state measurement and emission maxima observed at the shorter wavelength region disappeared because of the self-absorption as a result of the high concentrations. The radiolysis-induced emission intensities of **RA** were determined from the total amount of emission and summarized in Table 3. It is assumed that the emissions of **RA** mainly correspond to 9-cyanoanthracenyl moiety, which is known as an excellent fluorophore.[3]

All **RA** showed the fluorescence during pulse radiolysis in Bz. It was found that the emission intensity of **PA** was highest in Ar-saturated Bz. In addition, it was found that the emission intensity of **PA** at 10 mM was lower than that at 5 mM owing to the strong self-absorption. The emission intensity of **NEA** at 10 mM was also lower than that at 5 mM owing to the formation of the excimer. On the other hand, the emission intensities of **OEA** and **DEA** at 10 mM were higher than those at 5 mM

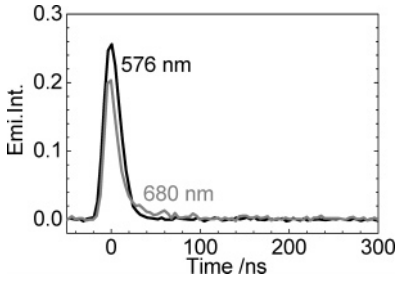


**FIGURE 3.** Time profiles of the emissions observed during the pulse radiolysis of **NEA** in Ar-saturated Bz (10 mM) at 576 and 680 nm.

owing to no intermolecular interaction. For **PEA**, little change of the emission intensity was observed when the concentration increased. In air-saturated Bz, the emission intensities of all **RA** decreased.

Figure 3 shows the time profiles of emissions observed at 576 (monomer emission) and 680 nm (excimer emission) of **NEA**. It is clearly indicated that the monomer and excimer were formed from the same precursor through the same reaction mechanism. **PEA** and **OEA** also showed the same emission behavior.

It was also found that the emission time profiles observed during the pulse radiolysis of **RA** in Ar-saturated Bz showed two components: short-lived with high emission intensity and long-lived with very low one. Even at a few microseconds after an electron pulse, the long-lived emission was observed and can be assigned to the delayed fluorescence resulting from triplet−triplet annihilation (T-route).[7c] The time profiles of emission observed during the pulse radiolysis of **RA** in air-saturated Bz (in the presence of dissolved oxygen) showed no long-lived emission component (Figure S1, Supporting Information). It is clearly shown that the long-lived emission component was quenched by oxygen. The quenching was observed for all **RA**, indicating that the "P-type" delayed fluorescence[9] was confirmed for **RA** in Bz during pulse radiolysis.

**Transient Absorption Spectra Observed during the Pulse Radiolysis of RA.** Figure 4 shows the transient absorption spectra observed during the pulse radiolysis of **RA** in Ar-saturated Bz. For D−A type **RA** (**OEA**, **NEA**, and **DEA**), the absorption bands at around 400−500 nm were not measured due to the strong ground-state absorption. The transient absorption was quenched during the pulse radiolysis of **RA** in air-saturated Bz. Thus, the transient absorption spectra, observed during the pulse radiolysis of **RA** in Ar-saturated Bz, are assigned mainly to $^3$**RA**$^*$.[7]

From the relationship between $-\Delta H°$ and the singlet excited-state energy calculated from the emission maxima of **RE** with the donor−acceptor structure, we have reported that the one-electron oxidation and reduction of **RE** can occur on the donor and acceptor moieties, and that the positive and negative charges of **RE**$^{\bullet+}$ and **RE**$^{\bullet-}$ are localized on the donor and acceptor moieties, respectively.[7] Since **RA** also has the donor−acceptor structure, the same charge localization is expected for **RA**$^{\bullet+}$ and **RA**$^{\bullet-}$. The absorption spectral shapes of **RA**$^{\bullet+}$ and **RA**$^{\bullet-}$ generated during the pulse radiolysis of **RA** in Ar-saturated 1,2-dichloroethane (DCE) and *N*,*N*-dimethylformamide (DMF), respectively, clearly indicated such charge localization. It is well

(9) (a) Liu, D. K. K.; Faulkner, L. R *J. Am. Chem. Soc.* **1977**, *99*, 4594. (b) Bohne, C.; Abuin, E. B.; Scaiano, J. C. *J. Am. Chem. Soc.* **1990**, *112*, 4226.

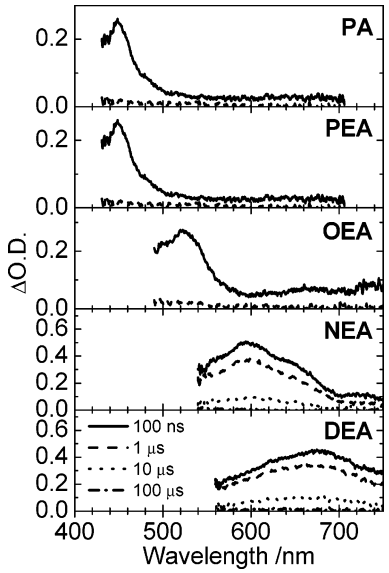


**FIGURE 4.** Time-resolved transient absorption spectra observed at time $t$ = 100 ns, 1, 10, and 100 $\mu$s after an electron pulse during the pulse radiolysis of **RA** in Ar-saturated Bz.

established that $\mathbf{M}^{\bullet+}$ and $\mathbf{M}^{\bullet-}$ are selectively generated during the pulse radiolysis of **M** in DCE[10] and in DMF,[12] respectively.

Figure 5 shows the transient absorption spectra observed during the pulse radiolysis of **RA** in Ar-saturated DCE. The absorption bands observed for all **RA** with a half-life time on the order of microseconds can be assigned to $\mathbf{RA}^{\bullet+}$. For $\mathbf{PEA}^{\bullet+}$, $\mathbf{NEA}^{\bullet+}$, and $\mathbf{DEA}^{\bullet+}$, a new absorption band was observed after the decay of the corresponding radical cation and remained even in the time scale longer than 100 $\mu$s, suggesting that $Cl^-$, generated from the initial radiolytic reactions of DCE, reacts with $\mathbf{RA}^{\bullet+}$ to give the product.[7] It should be noted that spectral shape of $\mathbf{RA}^{\bullet+}$ depends on molecular structure. Since the absorption spectrum of 9-cyanoanthracene$^{\bullet+}$ with two bands around 400−500 and 700−800 nm (Figure S1(a), Supporting Information) is different from those of $\mathbf{RA}^{\bullet+}$, the electronic property of the donor moiety affects the transient absorption of $\mathbf{RA}^{\bullet+}$, in which the positive charge is not localized on 9-cyanoanthracenyl moiety. For $\mathbf{PA}^{\bullet+}$ and $\mathbf{PEA}^{\bullet+}$, it seems that the positive charge is delocalized on two moieties. For $\mathbf{OEA}^{\bullet+}$, $\mathbf{NEA}^{\bullet+}$, and $\mathbf{DEA}^{\bullet+}$, two absorption bands were observed in the region of 600−800 nm. The absorption band around 650 nm corresponds mainly to phenyacetylene$^{\bullet+}$ with an absorption band at 622 nm.[11] The other strong absorption peak at 725, 680, and 760 nm for $\mathbf{OEA}^{\bullet+}$, $\mathbf{NEA}^{\bullet+}$, and $\mathbf{DEA}^{\bullet+}$, respectively, corresponds to the radical cation of the donor moieties. It has been reported that radical cations of anisole and *N*,*N*′-dimethyl-

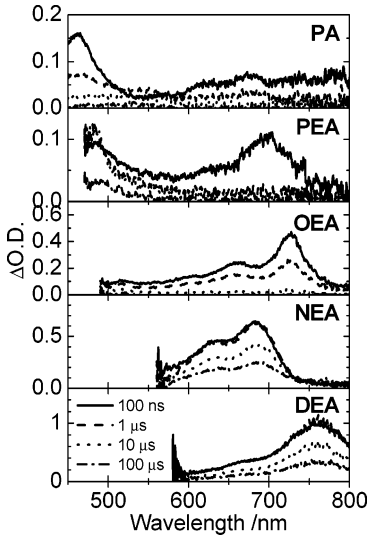


**FIGURE 5.** Time-resolved transient absorption spectra observed at time $t$ = 100 ns, 1, 10, and 100 $\mu$s after an electron pulse during the pulse radiolysis of **RA** in Ar-saturated DCE. The sample solutions were prepared in 5 mM concentration.

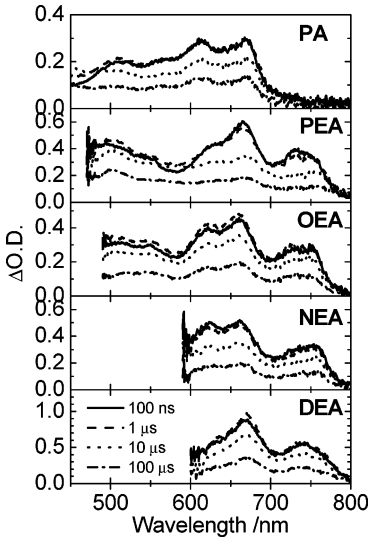


**FIGURE 6.** Time-resolved transient absorption spectra observed at time $t$ = 100 ns, 1, 10, and 100 $\mu$s after an electron pulse during the pulse radiolysis of **RA** in Ar-saturated DMF. The sample solutions were prepared in a 5 mM concentration.

aniline have broad and weak absorption bands in the region of 550−1500 and 550−700 nm, respectively.[11] The lifetimes of $\mathbf{PA}^{\bullet+}$ and $\mathbf{PEA}^{\bullet+}$ were shorter than one microsecond, while those of $\mathbf{OEA}^{\bullet+}$, $\mathbf{NEA}^{\bullet+}$, and $\mathbf{DEA}^{\bullet+}$ were in a few microseconds. This suggests that the reactivities of $\mathbf{PA}^{\bullet+}$ and $\mathbf{PEA}^{\bullet+}$ with $Cl^-$ are enhanced with increasing cationic character because of the positive charge delocalization including the 9-cyanoanthracenyl moiety in $\mathbf{PA}^{\bullet+}$ and $\mathbf{PEA}^{\bullet+}$, compared with $\mathbf{OEA}^{\bullet+}$, $\mathbf{NEA}^{\bullet+}$, and $\mathbf{DEA}^{\bullet+}$.

Figure 6 shows the transient absorption observed during the pulse radiolysis of **RA** in Ar-saturated DMF. The absorption bands observed for all **RA** with a half-life time on the order of microseconds can be assigned to $\mathbf{RA}^{\bullet-}$. It should be noted that $\mathbf{PA}^{\bullet-}$ has the absorption band at 500−700 nm, and other $\mathbf{RAs}^{\bullet-}$ with the ethynyl linkage have almost the same absorption band at 500−800 nm. It is suggested from the spectral shapes of $\mathbf{RA}^{\bullet-}$

(10) (a) Shida, T.; Hamill, W. H. *J. Chem. Phys.* **1966**, *44*, 2369, 2375, 3472. (b) Shida, T.; Kato, T. *Chem. Phys. Lett.* **1979**, *68*, 106. (c) Grimison, A.; Simpson, G. A. *J. Phys. Chem.* **1968**, *72*, 1776. (d) Ishida, A.; Fukui, M.; Ogawa, H.; Tojo, S.; Majima, T.; Takamuku, S. *J. Phys. Chem.* **1995**, *99*, 10808. (e) Majima, T.; Tojo, S.; Ishida, A.; Takamuku, S. *J. Org. Chem.* **1996**, *61*, 7793. (f) Majima, T.; Tojo, S.; Ishida, A.; Takamuku, S. *J. Phys. Chem.* **1996**, *100*, 13615.

(11) Shida, T. *Electronic Absorption Spectra of Radical Ions*; Physical Sciences Data 34; Elsevier Science Publishers: Amsterdam, 1988.

(12) (a) Honda, E.; Tokuda, M.; Yoshida, H.; Ogasawara, M. *Bull. Chem. Soc. Jpn.* **1987**, *60*, 851. (b) Huddleston, R. K.; Miller, J. R. *J. Phys. Chem.* **1982**, *86*, 2410. (c) Majima, T.; Fukui, M.; Ishida, A.; Takamuku, S. *J. Phys. Chem.* **1996**, *100*, 8913. (d) Majima T.; Tojo, S.; Takamuku, S. *J. Phys. Chem. A* **1997**, *101*, 1048.

that the negative charges localized mainly on 9-cyanoanthracenyl moiety because 9-cyanoanthracene$^{\bullet-}$ has an absorption band at around 500−700 nm (Figure S2(b), Supporting Information). For **RAs**$^{\bullet-}$ with the ethynyl linkage, the other absorption band appearing at 700−800 nm corresponds to the ethynyl linkage, because transient absorption spectra of radical anions of D−A type 9-cyanoanthracene derivatives without the ethynyl linkage, such as 9-cyano-10-(*p*-anisyl)anthracene, 9-cyano-10-(*p*-*N*,*N*-dimethylaminophenyl)anthracene, and 9-cyano-10-(*N*,*N*-di-*p*-anisylaminophenyl)anthracene, were observed to be similar to that of **PA**$^{\bullet-}$ with no absorption at 700−800 nm during the pulse radiolysis. The lifetimes for all **RA**$^{\bullet-}$ were in the order of several tens of microseconds, suggesting that the negative charges exist on 9-cyanoanthracenyl moiety and the ethynyl linker for **RA**$^{\bullet-}$.

No or little emission was observed during the pulse radiolysis of **RA** in DCE or DMF, suggesting that **RA**$^{\bullet+}$ or **RA**$^{\bullet-}$ itself does not emit light. In other words, both **RA**$^{\bullet+}$ and **RA**$^{\bullet-}$ must be formed at the same time in order to observe the emission. In Bz, however, no transient absorption band of **RA**$^{\bullet+}$ and **RA**$^{\bullet-}$ was observed immediately after an 8-ns electron pulse. Because Bz in the singlet excited state ($^1$Bz$^*$) has a short lifetime (12 ns), the singlet energy transfer to **RA** is possible only if the energy transfer rate constant is larger than $10^{10}$ $M^{-1}$ $s^{-1}$ even at high **RA** concentration (10 mM).[13] Since the diffusion-controlled rate constant in Bz is known to be $k_{diff} = 1.0 \times 10^{10}$ $M^{-1}$ $s^{-1}$, it is expected that the singlet energy transfer from $^1$Bz$^*$ to **RA** is limited only at the **RA** concentration larger than 10 mM. However, we observed the strong emission within the pulse duration (8 ns) during the pulse radiolysis of **RA** in Bz at low concentrations of 0.1−5 mM. Since the concentrations of generated $^3$**RA**$^*$ are estimated to be much lower than 10 mM (approximately 0.01 mM), emission observed within the 8-ns pulse duration cannot be generated from the triplet−triplet annihilation. Therefore, this emission must correspond to the charge recombination between **RA**$^{\bullet+}$ and **RA**$^{\bullet-}$, giving $^1$**RA**$^*$, $^3$**RA**$^*$, and $^1$(**RA**)$_2^*$ (for **PEA**, **OEA**, and **NEA**) within a pulse duration.[7] The emission intensity was decreased in the presence of $N_2O$ and $CH_3OH$ as the electron and hole scavengers, respectively, indicating that **RA**$^{\bullet+}$ and **RA**$^{\bullet-}$ are responsible to the emission during the pulse radiolysis of **RA** in Bz. It is also notable that $^1$(**RA**)$_2^*$ is not generated with the steady-state experiment even at high concentration.

**Emission Mechanism.** In Bz, $-\Delta H°$ can be expressed by simplified eq 3,

$$-\Delta H° = E_{ox} - E_{red} + 0.13 \text{ eV} \quad (3)$$

where $E_{ox}$ and $E_{red}$ are the oxidation and reduction potentials of **RA** in $CH_2Cl_2$ (Table 2). $-\Delta H°$ values for **RA** in Bz were shown in Table 4 with the singlet excited-state energy calculated from the emission maxima ($E'_{S1}$) during pulse radiolysis.

Table 4 shows that $-\Delta H°$ values for **RA** are larger than $E'_{S1}$, suggesting that the energy available in the charge recombination is sufficient to populate the $S_1$ state for all **RA**. The relation between $-\Delta H°$ and $E'_{S1}$ can explain that the short-lived emission component observed for **RA** is resulted from $^1$**RA**$^*$ which was formed through the direct charge recombination between **RA**$^{\bullet+}$ and **RA**$^{\bullet-}$ (S-route), and that the long-lived emission component is from $^1$**RA**$^*$ formed via T-route. The relation of $-\Delta H°$, $E'_{S1}$, and $E_{S1}$ (determined at the concentration of $10^{-5}$ M with the steady-state measurements) was discussed in the Supporting Information.

**TABLE 4. Annihilation Enthalpy Changes ($-\Delta H°$) and the Singlet Excited-State Energy Calculated from the Emission Maxima ($E'_{S1}$) during the Pulse Radiolysis of RA in Bz**

| RA | $-\Delta H°$, eV | $E'_{S1}$, eV[a] |
|---|---|---|
| **PA** | 3.48 | 2.65 |
| **PEA** | 2.51 | 2.51 |
| **OEA** | 2.55 | 2.45 |
| **NEA** | 2.45 | 2.18 |
| **DEA** | 2.32 | 2.07 |

[a] Estimated from the peak wavelength of the emission spectra observed during pulse radiolysis (5 mM).

The transient absorption spectral shapes of **PA**$^{\bullet+}$ and **PEA**$^{\bullet+}$ showed that the positive charge is delocalized on two moieties of **RA**$^{\bullet+}$, while those of **PA**$^{\bullet-}$ and **PEA**$^{\bullet-}$ showed that the negative charge is localized on 9-cyanoanthracenyl moiety of **RA**$^{\bullet-}$ (Figures 4 and 5). Therefore, it is suggested that the charge recombination between **PA**$^{\bullet+}$ with delocalized charge and **PA**$^{\bullet-}$ with localized one on 9-cyanoanthracenyl moiety occurs to give $^1$**PA**$^*$ during pulse radiolysis in Bz. It has been indicated by the DFT calculation that **PEA** has planar geometry owing to the presence of the ethynyl linkage although **PA** has a twisted geometry.[3] Thus, for **PEA**, both $\pi$-stacking interaction between two 9-cyanoanthracenyl moieties and between two phenyl moieties are possible in an encounter complex of **PEA** with the proximally parallel geometry during the charge recombination between **PEA**$^{\bullet+}$ and **PEA**$^{\bullet-}$ to give the monomer and excimer emissions (Schemes 2 and 4).

For the D−A type **RA**, transient absorption spectra of **RA**$^{\bullet+}$ showed that the positive charge was localized on the donor moieties. On the other hand, the transient absorption spectra of **RA**$^{\bullet-}$ showed that the negative charges of all **RA**$^{\bullet-}$ were mainly localized on 9-cyanoanthracenyl moieties. Thus, the emissive ICT state ($^1$(A$^{\bullet-}$-D$^{\bullet+}$)$^*$) can be formed by the charge recombination between **RA**$^{\bullet+}$ and **RA**$^{\bullet-}$ as shown in Schemes 3 and 4. Therefore, it is suggested that the charge recombination between **RA**$^{\bullet+}$ and **RA**$^{\bullet-}$ with localized charges occurs to give $^1$**RA**$^*$ with the ICT character and $^1$(**RA**)$_2^*$ (for **OEA** and **NEA**) which emit lights during the pulse radiolysis of D−A type **RA** in Bz. It has been reported that D−A type **RA** has twisted geometry. In addition, weak ICT was indicated for $^1$**OEA**$^*$, and strong ICT was for $^1$**NEA**$^*$ and $^1$**DEA**$^*$.[3] Thus, it is suggested that both $\pi$-stacking interactions between two 9-cyanoanthracenyl moieties and between two *p*-anisyl moieties are possible for the encounter complex of **OEA** with the proximally parallel geometry during the charge recombination between **OEA**$^{\bullet+}$ and **OEA**$^{\bullet-}$ to give the monomer and excimer emission. For **NEA**, it is expected that **NEA**$^{\bullet+}$ and **NEA**$^{\bullet-}$ collide neck-to-neck to generate the excimer in which two 9-cyanoanthracenyl moieties are stacked in the face-to-face configuration with two dimethylaminophenyl moieties projecting perpendicularly away from each other due to the twisted geometry (Scheme 3). For **DEA** with strong and bulky donor substituent, a considerably twisted structure is assumed to give $^1$**DEA**$^*$ with strong ICT character but not $^1$(**DEA**)$_2^*$ because of the bulky donor substituent.

Thus, it is clarified that the charge recombination between **RA**$^{\bullet+}$ and **RA**$^{\bullet-}$ occurs to give $^1$**RA**$^*$ and $^1$(**RA**)$_2^*$ (for **PEA**, **OEA**, and **NEA**) during the pulse radiolysis of **RA** in Bz. In addition, the delayed fluorescence (long-lived emission component with very low intensity) was also observed in Ar-saturated Bz. This delayed fluorescence was quenched by

(13) Mohan, H.; Brede, O.; Mittal, J. P. *J. Photochem. Photobiol., A* **2001**, *140*, 191.

**SCHEME 2**

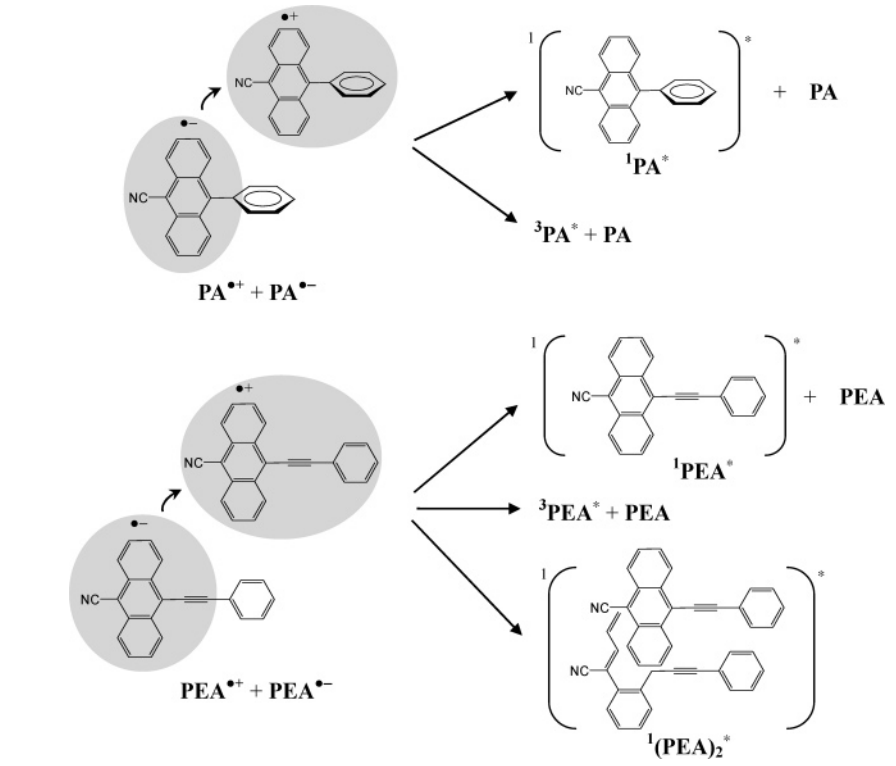


**SCHEME 3**

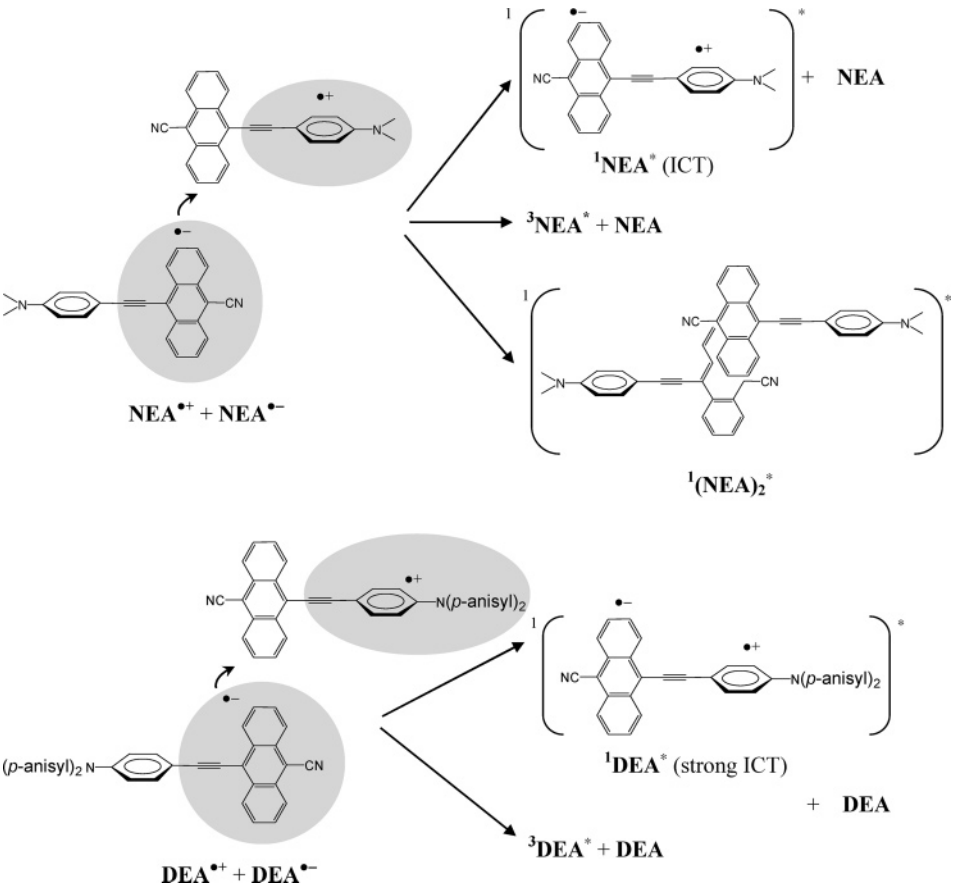


oxygen, indicating that it was derived from the triplet−triplet annihilation (T-route). The mechanism of the delayed fluorescence during the pulse radiolysis of **RA** in Bz is summarized as Scheme 4. The transient absorption spectral shapes of $\mathbf{PA}^{\bullet+}$ and $\mathbf{PEA}^{\bullet+}$ showed that the positive charge is delocalized on two moieties of $\mathbf{RA}^{\bullet+}$, while $\mathbf{PA}^{\bullet-}$ and $\mathbf{PEA}^{\bullet-}$ showed that the

**SCHEME 4. Mechanism of the Emission during the Pulse Radiolysis of D−A Type RA in Bz**[a]

$$e^- + \mathbf{RA} \rightarrow \mathbf{RA}^{\bullet -}$$

$$Bz^{\bullet +} + \mathbf{RA} \rightarrow Bz + \mathbf{RA}^{\bullet +}$$

$$\mathbf{RA}^{\bullet +} + \mathbf{RA}^{\bullet -} \rightarrow {}^1\mathbf{RA}^* + \mathbf{RA} \text{ and } {}^3\mathbf{RA}^* + \mathbf{RA}$$

$$\mathbf{RA}^{\bullet +} + \mathbf{RA}^{\bullet -} \rightarrow {}^1\mathbf{RA}^* + \mathbf{RA}, {}^3\mathbf{RA}^* + \mathbf{RA}, \text{ and } {}^1(\mathbf{RA})_2^* \text{ (for PEA, OEA, and NEA)}$$

$${}^3\mathbf{Bz}^* + \mathbf{RA} \rightarrow \mathbf{Bz}^3 + \mathbf{RA}^*$$

$${}^3\mathbf{RA}^* + {}^3\mathbf{RA}^* \rightarrow {}^1\mathbf{RA}^* + \mathbf{RA}$$

$${}^1\mathbf{RA}^* \rightarrow \mathbf{RA} + h\nu_f$$

$${}^1\mathbf{RA}^* \rightarrow \mathbf{RA} + h\nu_{df}$$

$${}^1(\mathbf{RA})_2^* \rightarrow 2\,\mathbf{RA} + h\nu_{ex} \text{ (for PEA, OEA, and NEA)}$$

[a] $h\nu_f$, $h\nu_{ex}$, and $h\nu_{df}$ denote fluorescence from monomer, excimer, and P-type delayed emission derived from triplet−triplet annihilation, respectively. For D−A Type **RA**, $\mathbf{RA}^{\bullet -}$ = $A^{\bullet -}$−D, $\mathbf{RA}^{\bullet +}$ = A−$D^{\bullet +}$, ${}^1\mathbf{RA}^*$ = ${}^1(A^{\bullet -}-D^{\bullet +})^*$

negative charge is localized on 9-cyanoanthracenyl moiety of $\mathbf{RA}^{\bullet -}$. It is suggested that the positive charge of the D−A type $\mathbf{RA}^{\bullet +}$ ($\mathbf{OEA}^{\bullet +}$, $\mathbf{NEA}^{\bullet +}$, and $\mathbf{DEA}^{\bullet +}$) is localized on donor moieties, and that the negative charge of $\mathbf{RA}^{\bullet -}$ ($\mathbf{OEA}^{\bullet -}$, $\mathbf{NEA}^{\bullet -}$, and $\mathbf{DEA}^{\bullet -}$) is localized on acceptor moieties. Thus, the charge recombination between $\mathbf{RA}^{\bullet +}$ and $\mathbf{RA}^{\bullet -}$ with localized charges occurs to give ${}^1\mathbf{RA}^*$ with ICT character and/or ${}^1(\mathbf{RA})_2^*$ which emit lights during the pulse radiolysis of D−A type **RA** in Bz.

## Conclusions

Several substituted **RA** with or without donor−acceptor character showed monomer and excimer emissions during pulse radiolysis in Bz. The emission is suggested to be originated from ${}^1\mathbf{RA}^*$ generated by the charge recombination between $\mathbf{RA}^{\bullet +}$ and $\mathbf{RA}^{\bullet -}$ which are yielded from the initial radiolytic reaction in Bz. This mechanism is reasonably explained by the fact that $-\Delta H°$ values (2.32−3.48 eV) estimated for the charge recombination between $\mathbf{RA}^{\bullet +}$ and $\mathbf{RA}^{\bullet -}$ are sufficiently larger than the singlet excited-state energy calculated from the emission maxima ($E'_{S1}$) of **RA** (2.07−2.65 eV). **PA** and **DEA** showed only monomer emission during pulse radiolysis in Bz. On the other hand, **PEA** and **NEA** showed both monomer and excimer emissions, leading to a reduction in the emission efficiency.

Although the introduction of the ethynyl linkage for **RA** provides the broad emission which covers the visible region, that also causes aggregation to form excimer, leading to a reduction in the emission efficiency. However, **RA** with a strong electron donor substituent (**DEA**) exhibits strong ICT (${}^1(A^{\bullet -}-D^{\bullet +})^*$) and the excimer structure is not formed due to the twisted geometry, precluding reduction in the emission efficiency even at high concentration. The emission property of this type of $\pi$-conjugated D−A type molecule can be useful information for developing electroluminescent materials for OLEDs.

## Experimental Section

**Measurements of Photophysical and Electrochemical Properties.** UV spectra were recorded in Bz with a UV/visible spectrometer using a transparent rectangular cell made from quartz (1.0 × 1.0 × 4.0 cm, path length of 1.0 cm). Fluorescence spectra were measured with a spectrofluorometer. The oxidation and reduction potential values were measured with cyclic voltammograms (CV). Using a setup consisting of a spectrofluorometer and voltammograph with a PC interface, ECL emissions were measured.[2,3] The fluorescence quantum yields ($\phi_{fl}$) were determined by using coumarin 106 standard ($\phi_{fl}$ = 0.57 in MeOH, $\lambda_{ex}$ =390 nm). The fluorescence lifetime ($\tau_{fl}$) measurement was carried out using a single photon counter.

**Pulse Radiolysis**. Pulse radiolysis experiments were performed using an electron pulse (28 MeV, 8 ns, 0.87 kGy per pulse) from a linear accelerator at Osaka University. All the sample solutions were prepared in a 5 and 10 mM concentration in Bz in a rectangular quartz cell (0.5 × 1.0 × 4.0 cm, path length of 1.0 cm). These solutions were saturated with Ar gas by bubbling with it for 10 min at room temperature before irradiation. The kinetic measurements were performed using a nanosecond photoreaction analyzer system. The monitor light was obtained from a pulsed 450-W Xe arc lamp, which was operated by a large current pulsed-power supply that was synchronized with the electron pulse. The monitor light was passed through an iris with a diameter of 0.2 cm and sent into the sample solution at a perpendicular intersection to the electron pulse. The monitor light passing through the sample was focused on the entrance slit of a monochromator and detected with a photomultiplier tube. The transient absorption and emission spectra were measured using a photodiode array with a gated image intensifier as a detector. To avoid pyrolysis of the sample solution by monitor light, a suitable cutoff filter was used.

**Acknowledgment.** We thank the members of the Radiation Laboratory of SANKEN, Osaka University, for running the linear accelerator. This work has been partly supported by a Grant-in-Aid for Scientific Research (Project 17105005, Priority Area (417), 21st Century COE Research, and others) from the Ministry of Education, Culture, Sports, Science and Technology (MEXT) of the Japanese Government.

**Supporting Information Available:** Time profiles of the emission intensities at 576 nm observed during the pulse radiolysis of **NEA** in Ar- and air-saturated Bz (5 mM). Transient absorption spectra observed during the pulse radiolysis of 9-cyanoanthracene (5 mM) in Ar-saturated DCE, and DMF. The relation of $-\Delta H°$, $E_{S1}$, and $E'_{S1}$ values. This material is available free of charge via Internet at http://pubs.acs.org.

JO060929N